

Braneworld Black Bounce to Transversable Wormhole

Tiago M. Crispim ^{a,1} Milko Estrada ^{b,2} C. R. Muniz^{c,3} and G. Alencar ^{d1}

¹*Departamento de Física, Universidade Federal do Ceará,*

Caixa Postal 6030, Campus do Pici, 60455-760 Fortaleza, Ceará, Brazil

²*Facultad de Ingeniería y Empresa, Universidad Católica Silva Henríquez, Chile*

³*Universidade Estadual do Ceará (UECE), Faculdade de Educação,*

Ciências e Letras de Iguatu, 63500-000, Iguatu, CE, Brazil.

(Dated: May 15, 2024)

Abstract

We provide a $5D$ generalization of the Hawking *et al.* black string in a Randall Sundrum setup. The embedded $4D$ geometry corresponds to the Simpson-Visser (SV) spacetime, which can represent a traversable wormhole, a one-way wormhole, or a regular black hole. To achieve this, we linearly deform both the bulk geometry and the bulk matter distribution with respect to a coupling constant. These deformations induce a transition from a $5D$ vacuum AdS distribution to an anisotropic distribution. The latter results in the induced geometry on the brane transitioning from a singular Schwarzschild spacetime to a regularized SV spacetime. Since there are no sources or matter fields on the brane, we can assert that the induced SV geometry on the brane arises from the influence of geometrical and matter deformations in the bulk. Thus, the central singularity is suppressed. We determine the cases where the energy conditions are either satisfied or violated. Our spacetime is asymptotically radial AdS, which is intriguing given the absence of a global AdS box that would prevent instability under larger wavelength perturbations. Therefore, it is no longer appropriate to claim that instability exists for very small perturbations near the AdS horizon.

^a E-mail: tiago.crispim@fisica.ufc.br

^b E-mail: mestrada@ucsh.cl

^c E-mail: celio.muniz@uece.br

^d E-mail: geova@fisica.ufc.br

I. INTRODUCTION

Over the last few years, General Relativity (GR) has gained significant attention. This is due to the present era of high-precision measurements of black holes and cosmology, which allowed the direct measurement of gravitational waves by LIGO and VIRGO, the image of supermassive black holes by EHT, and precise measurements of the Λ CDM parameters [1–7]. This opens a new window to detect extra dimensions, and the Randall-Sundrum model (RS) have garnered increased interest. It has many attractive features, explaining why gravity is weaker than the other forces of nature, the hierarchy problem, beyond being an alternative to compactification [8, 9]. RS models have also garnered interest in testing the potential existence of extra dimensions using data obtained from gravitational experiments [10, 11].

The RS model involves the embedding of $4D$ flat branes, *i.e.*, whose geometry corresponds to Minkowski spacetime. Since its inception, various generalizations of the Randall-Sundrum model, featuring different types of four-dimensional geometries including black holes and wormholes, have emerged. The approach to studying these generalizations is primarily based on two main approximations: one originates from the brane, and the other from the bulk. In the former, the four-dimensional black holes or wormholes are constructed by studying the equations of motion induced on the brane [12]. Some examples in references [13–16]. However, this methodology does not fully allow for testing the influence of bulk geometry on the physical and geometric behavior of the four-dimensional geometry. Regarding the latter, the second approach constructs spacetimes directly from the bulk, and the brane equations are derived from there. See [17, 18]. The approach embraced in this study aligns with the latter. See other recent and different applications to braneworld models in references [19–21].

Soon later Hawking *et al.* demonstrated that the brane geometry can correspond to a four-dimensional Schwarzschild black hole embedded in a five-dimensional AdS spacetime, also known as the black strings (BS) solution [22]. It is important to mention that analysis of observations of the shadows of M87* has provided indications that the induced geometry on the brane could represent both ultra-compact objects and wormholes. In particular, reference [23], studying the embedding of such objects, demonstrated that the braneworld scenario fits better with the observed shadow and the diameter of the image of Sgr A* compared to the corresponding situation in general relativity. Even though wormholes, in general, require exotic matter to remain stable, in the presence of extra dimensions such is not the case. Therefore, they showed that the wormhole solution considered does not require exotic matter on the brane. Thus, this reason renewed the

interest in embedding other types of geometries different from the Schwarzschild vacuum solution, such as wormholes or regular black holes.

A notable physical consequence is that black string solutions in asymptotically flat space are unstable to wavelength perturbations [24]. However, as mentioned in reference [22], an AdS spacetime acts as a confining box that prevents the development of fluctuations with wavelengths much greater than l , thereby averting this type of instability. Other characteristics of the model discussed in reference [22] include that the Kretschmann invariant diverges at the origin of the radial coordinate and the infinity of the extra dimension (the so-called AdS horizon). Thus, at these two locations, the laws of physics cease to operate.

In another direction, a theoretical value of the AdS radius was estimated in the RS framework from recent data from near-simultaneous detection of the GW event GW170817 from the LIGO/Virgo collaboration and its electromagnetic counterpart, the short gamma-ray burst GRB170817A detected by the Fermi Gamma-ray Burst Monitor and the International Gamma-Ray Astrophysics Laboratory Anti-Coincidence Shield spectrometer, [10]. This estimation revealed that the results obtained are inconsistent with observations of the solar system at millimeter scales. Therefore, the bulk could be described by a source other than a vacuum represented by an AdS cosmological constant.

On the other hand, in reference [25], a method for regularizing the Schwarzschild spacetime was proposed by introducing a regularization parameter a^2 . Depending on the value of a , the four-dimensional spacetime could represent a traversable wormhole (TWH), a one-way wormhole (OWWH) with an extremal null throat at $r = 0$, or a regular black hole (RBH). The method has been used recently to regularize cylindrical black holes, such as BTZ and $4d$ black strings [26–31]. Therefore, it is interesting to investigate whether the same is true for $5D$ black strings. Another feature of the SV solution is that a source is necessary; therefore, it is not a vacuum solution. This is very attractive since, as said above, the bulk must be described by a source other than a vacuum.

Finally, in recent years, there has been considerable attention drawn to the fact that the deformation of the Einstein tensor and the matter content within the energy-momentum tensor can modify the geometry of an object [32]. In this work, we will study the geometric characteristics that the five-dimensional bulk and the energy-momentum distribution in the five-dimensional bulk must possess for the induced geometry on the brane to correspond to TWH, an OWWH, or an RBH in the SV set-up. We analyze the locations where the solution is regular and investigate the

energy conditions. We discuss the effects of deformations in the geometry and matter of the $5D$ bulk on the induced $4D$ geometry on the brane and speculate about the nature of the new sources of matter derived from this deformation. The stability of the obtained solutions will be studied considering the sound speed within the source on the brane, as well as the potential presence of an AdS box that may prevent instability under wavelength perturbations.

II. REVISITING HAWKING ET AL. MODEL

One way of constructing a black hole solution in a braneworld scenario was proposed by Hawking *et al.* in reference [22]. The focus of the paper is the AdS singularity. However, since we are also interested in the Black string stability, we will revisit the authors' results to include this. They began with the Randall-Sundrum metric expressed in terms of the new coordinate $z = le^{y/l}$

$$ds^2 = \frac{l^2}{z^2}(\eta_{\mu\nu}dx^\mu dx^\nu + dz^2). \quad (1)$$

The authors constructed a black string solution in five dimensions by replacing the Minkowski element in the metric (1) with

$$ds^2 = \frac{l^2}{z^2}[-U(r)dt^2 + U(r)^{-1}dr^2 + r^2(d\theta^2 + \sin^2\theta d\phi^2) + dz^2], \quad (2)$$

with $U(r) = 1 - \frac{2M}{r}$, which describes a $4d$ Schwarzschild line element. M is a constant associated with the mass of the four-dimensional black hole embedded into an extra dimension. The coordinates take on values in the following ranges: $t \in (-\infty, +\infty)$, $r \in [0, +\infty)$, $\phi \in [0, 2\pi]$, $\theta \in [0, \pi]$, and $z \in (-\infty, +\infty)$. Soon latter, it was shown that the Hawking is unstable under linear perturbations [33].

An interesting aspect of this geometry is that it exhibits two singularities: one located along $r = 0$, akin to a Schwarzschild black hole, and another singularity at $z = \infty$. These characteristics can be demonstrated by analyzing the Kretschmann scalar, which is given by:

$$R_{MNPQ}R^{MNPQ} = \frac{1}{l^4} \left(40 + \frac{48M^2z^4}{r^6} \right). \quad (3)$$

It's easy to see that $R_{MNPQ}R^{MNPQ}$ diverges at the AdS horizon ($z = \infty$) and the singularity of the black hole ($r = 0$). If one persists in demanding the Schwarzschild metric on the brane, albeit with a standard AdS horizon, the consequence is the necessity of accommodating matter within the bulk [34].

Next, to analyze this singularity, the authors consider the behavior of geodesics. By considering the where affine parameter λ , the geodesic equation for the z coordinate ($\theta = \pi/2$) is given by

$$\frac{d}{d\lambda} \left(\frac{1}{z^2} \frac{dz}{d\lambda} \right) = \frac{\sigma}{zl^2}, \quad (4)$$

where $\sigma = 0, 1$ are for null and time-like geodesics. We are interested in solutions in which z can reach the singularity. For null and time-like geodesics, they are given by

$$z = -\frac{z_1 l}{\lambda}, z = -z_1 \csc(\lambda/l). \quad (5)$$

In both cases, z_1 is a constant fixed so that $\lim_{\lambda \rightarrow 0^-} z \rightarrow \infty$. This can be used to analyze the radial direction. Next, the authors introduce the parameters

$$\nu = -\frac{z_1^2}{\lambda}, \nu = -(z_1^2/l) \cot(\lambda/l) \quad (6)$$

for null and time-like geodesics and define new coordinates and constants

$$r = z_1 r/l, \bar{E} = z_1 E/l, \bar{L} = z_1^2 L/l^2, \bar{M} = z_1 M/l. \quad (7)$$

This leaves the radial equation in the form

$$\left(\frac{d\bar{r}}{d\nu} \right)^2 + \left(1 + \frac{\bar{L}^2}{\bar{r}^2} \right) \left(1 - \frac{2\bar{M}}{\bar{r}} \right) = \bar{E}^2. \quad (8)$$

where \bar{M} is the ADM mass for an observer at $z = z_0 = l^2/z_1$. With the above equation, the authors conclude that bound geodesics are divergent at the AdS boundary, but the unbounded ones are not.

In order to conclude about singularity, they calculate the Riemann scalar in a reference frame that propagates parallel to the geodesics. Let the tangent vector to these geodesics with $L = 0$ be given by

$$u^M = \left(\frac{Ez^2}{U(r)l^2}, \frac{z^2}{l^2} \sqrt{E^2 - \frac{l^2}{z_1^2} U(r)}, 0, 0, \frac{z}{l} \sqrt{\frac{z^2}{z_1^2} - 1} \right), \quad (9)$$

The unit normal vector to the geodesic n^M , which is parallel propagated along it, is given by

$$n^N = \left(-\frac{zz_1}{l^2 U(r)} \sqrt{E^2 - \frac{l^2}{z_1^2} U(r)}, -\frac{Ez_1 z}{l^2}, 0, 0, 0 \right). \quad (10)$$

When is straightforward to check that $u^P \nabla_P n^Q = 0$. Thus, by calculating one of the curvature components in this reference frame, we obtain

$$R_{(u)(n)(u)(n)} = R_{MNPQ} u^M n^N u^P n^Q = \frac{1}{l^2} \left(1 - \frac{z^4}{z_1^2} \frac{2M}{r^3} \right), \quad (11)$$

which diverges along the geodesic to $\lambda \rightarrow 0^-$. The same conclusion is obtained considering $\bar{L} = 0$ in Eq.(8). We get

$$\left(\frac{d\bar{r}}{d\nu}\right)^2 + \left(1 - \frac{2\bar{M}}{\bar{r}}\right) = \bar{E}^2, \quad (12)$$

and, as expected, the solution diverges at $\bar{r} = 0$.

On the other hand, following the idea of Randall Sundrum, a mass parameter M located on a brane located at $y = y_0$ in an effective 4D theory is given by $M_e = \exp(-y_0/l)M$. Following reference [22], under a change of coordinates $w = z - z_0$, the metric maintains its structure, and the wall also could be located at $w = 0 \rightarrow z = z_0$. Thus, using $z = le^{y/l}$, the mass measured by an inhabitant of the wall at $z = z_0$ would be $M_e = Ml/z_0$. This implies that the proper radius of the horizon in five dimensions is $r_e = 2M_e$. Assuming that the AdS radius l is on the order of the Planck length, it should hold that $M/z_0 \gg 1$ to be consistent with astrophysical data.

It is well known that black string solutions in asymptotically flat space are unstable to wavelength perturbations [24]. In the case of RS black holes, as indicated by reference [22], an AdS spacetime acts like a confining box that prevents fluctuations with wavelengths much greater than l from developing, thus preventing the occurrence of this type of instability. Thus, if the curvature scalar $R = -20/l^2$ is very small, the AdS curvature is negligible, and the space-time behaves like a flat space. This means that the black string solution will be unstable to perturbations with wavelengths on the order of the horizon radius $r_e = \frac{2Ml}{z_0}$ such that $\frac{r_e}{l} = \frac{2M_e}{l} = \frac{2M}{z_0} \ll 1$. In other words, for very large values of z , such perturbations will fit into the AdS box, so instability could occur near the AdS horizon. However, for $\frac{2M}{z_0} \gg 1$, the potential instability would occur at wavelengths much larger than l , i.e., $\frac{r_e}{l} = \frac{2M}{z_0} \gg 1$, and, therefore, the AdS curvature prevents instability. Otherwise, an instability can occur, but if it does, it must do so at smaller wavelengths. Thus, the black string solution is stable far from the AdS horizon but potentially unstable near it. The question was settled when it was shown that RS black holes are unstable under linear perturbations [33].

A simple way to study instability is by the use of squared sound speed [35] along a direction (coordinate) i . It is given by

$$(v_s^i)^2 = \frac{d \langle p \rangle}{d\rho}, \quad (13)$$

where $\langle p \rangle$ is the average pressure. To ensure stability in the solution, the speed of sound must satisfy $(v_s^i)^2 \geq 0$, with an additional constraint of $v_s^i < 1$ in order to be physical. We, therefore, conclude that the solution is unstable for the Hawing model since $d \langle p \rangle / d\rho = -1$. We will use this method to study the instability of the black-bounce RS black hole.

III. SIMPSON-VISSER REGULARIZATION METHOD APPLIED TO HAWKING MODEL

To eliminate the radial singularity of equations (3), (11) and (12), we can consider the Simpson-Visser regularization [25] on the Schwarzschild line element 2. Therefore, now consider the metric given by

$$ds^2 = \frac{l^2}{z^2} [-\mathcal{U}(r)dt^2 + \mathcal{U}(r)^{-1}dr^2 + (r^2 + a^2)(d\theta^2 + \sin^2 \theta d\phi^2) + dz^2], \quad (14)$$

where $\mathcal{U}(r) = 1 - 2M/\sqrt{r^2 + a^2}$ and the coordinates now take on values in the ranges $t \in (-\infty, +\infty)$, $r \in [0, +\infty)$, $\phi \in [0, 2\pi]$, $\theta \in [0, \pi]$ and $z \in (-\infty, +\infty)$.

We can analyze the causal structure of this geometry by taking $\theta = \pi/2$, $\phi = 0$, $z = cte = z_0$, and $ds = 0$, from which we obtain the following expression for dr/dt

$$\frac{dr}{dt} = \pm \left(1 - \frac{2M}{\sqrt{r^2 + a^2}} \right). \quad (15)$$

This is the same expression obtained by [25]. Thus, the conclusions are similar, i.e.:

- If $a > 2M$, then for any value of r , $\frac{dr}{dt} \neq 0$, and therefore we have a braneworld two-way traversable wormhole;
- If $a = 2M$, $\frac{dr}{dt} \rightarrow 0$ when $r \rightarrow 0$, which shows that at $r = 0$ we have a horizon. Thus, we have a braneworld one-way wormhole.
- If $a < 2M$, $\frac{dr}{dt} = 0$ for $r_h = \pm\sqrt{(2M)^2 - a^2}$, and so we have a braneworld regularized black hole with the horizon at r_h .

As a simplification, we can also make a coordinate change in the radial direction given by $\tilde{r}^2 = r^2 + a^2$. With this, the metric takes the form

$$ds^2 = \frac{l^2}{z^2} \left[- \left(1 - \frac{2M}{\tilde{r}} \right) dt^2 + \frac{d\tilde{r}^2}{\left(1 - \frac{2M}{\tilde{r}} \right) \left(1 - \frac{a^2}{\tilde{r}^2} \right)} + \tilde{r}^2(d\theta^2 + \sin^2 \theta d\phi^2) + dz^2 \right], \quad (16)$$

where now $t \in (-\infty, +\infty)$, $\tilde{r} \in [a, +\infty)$, $\phi \in [0, 2\pi]$, $\theta \in [0, \pi]$ and $z \in (-\infty, +\infty)$.

In another direction, for the non-zero components of the Einstein tensor, we have

$$\begin{aligned} G_0^0 &= \frac{1}{l^2} \left(6 + \frac{a^2 z^2 (\tilde{r} - 4M)}{\tilde{r}^5} \right); & G_1^1 &= \frac{1}{l^2} \left(6 - \frac{a^2 z^2}{\tilde{r}^4} \right); \\ G_2^2 &= G_3^3 = \frac{1}{l^2} \left(6 + \frac{a^2 z^2 (\tilde{r} - M)}{\tilde{r}^5} \right); & G_4^4 &= \frac{1}{l^2} \left(6 + \frac{a^2 z^2 (\tilde{r} - 3M)}{\tilde{r}^5} \right). \end{aligned} \quad (17)$$

Note that all components of the Einstein tensor can be written as:

$$G_B^A = (G_B^A)_{\text{seed}} + a^2 \cdot (\text{Geometric Deformation})\delta_B^A. \quad (18)$$

Therefore, the coupling a^2 induces a linear deformation of the bulk geometry, with the 5D Hawking black string [22] as a seed solution. This also shows that a linear deformation of the 5D energy-momentum tensor is necessary (as detailed below in equation 36).

$$T_B^A = (T_B^A)_{\text{seed}} + a^2 \cdot (\text{Matter Deformation})\delta_B^A. \quad (19)$$

This results from the induced geometry on the brane transitioning from a Schwarzschild singular spacetime to a regularized SV spacetime. It can be interpreted as a matter deformation, generating a transition from a vacuum distribution, characterized by the 5D cosmological constant, to an anisotropic distribution. It is worth mentioning that as the radial coordinate tends to infinity, all components of the geometrical deformation of the Einstein tensor vanish. This is consistent with the observation that, in this limit, spacetime behaves as AdS₅.

It is worth noting that linear deformations of geometry and matter have attracted considerable attention in recent years through the Gravitational decoupling algorithm [32], where, in a superficial explanation, the motion equations are decoupled to obtain new solutions. Notably, the distribution of matter in the bulk doesn't globally exhibit a negative cosmological constant. We also expect that the radial singularity is excluded and, finally, the parameter a will influence the stability of the background metric. The investigation singularities will be done in the next subsections. The study of energy conditions and stability will be left to the next sections.

A. Ricci and Kretschmann invariants

A good way to study singularity is by evaluating the Ricci and Kretschmann invariants. They are respectively given by

$$R = -\frac{1}{l^2} \left(20 + \frac{2a^2 z^2 (\tilde{r} - 3M)}{\tilde{r}^5} \right). \quad (20)$$

and

$$\begin{aligned} \mathcal{K} = \frac{1}{l^4} \left[40 + \frac{48M^2 z^4}{\tilde{r}^6} + a^2 \left(-\frac{24M z^2}{\tilde{r}^5} + \frac{8z^2}{\tilde{r}^4} - \frac{144M^2 z^4}{\tilde{r}^8} + \frac{32M z^4}{\tilde{r}^7} \right) \right. \\ \left. + a^4 \left(\frac{132M^2 z^4}{\tilde{r}^{10}} - \frac{64M z^4}{\tilde{r}^9} + \frac{12z^4}{\tilde{r}^8} \right) \right] \quad (21) \end{aligned}$$

It is important to note that, as expected, taking $a \rightarrow 0$ returns (3). Here we assume the general case where $a \neq 0$, so that we have the following asymptotic behaviors

$$\lim_{\tilde{r} \rightarrow a} R = -\frac{1}{l^2} \left(20 + \frac{2z^2(a - 3M)}{a^3} \right), \quad (22)$$

$$\lim_{\tilde{r} \rightarrow a} \mathcal{K} = \frac{1}{l^4} \left(40 + \frac{8z^2}{a^2} - \frac{24Mz^2}{a^3} + \frac{12z^4}{a^4} - \frac{32Mz^4}{a^5} + \frac{36M^2z^4}{a^6} \right), \quad (23)$$

$$\lim_{\tilde{r} \rightarrow \infty} R = -\frac{20}{l^2}, \quad (24)$$

$$\lim_{\tilde{r} \rightarrow \infty} \mathcal{K} = \frac{40}{l^2}. \quad (25)$$

From equations (22), (23), we can deduce that the spacetime $5D$ is regular at the origin $r = 0$ (or $\tilde{r} = a$), unlike (3), which is singular at the origin. On the other hand, from equations (24), (25), we observe that at the infinite of the radial coordinate, the values of the scalars Ricci and Kretschmann corresponding to an AdS space are recovered. Thus, unlike [22], which has a global AdS behavior, in our case such behavior only occurs locally at the radial coordinate's asymptote.

In addition, \mathcal{K} continues to diverge in $z \rightarrow \infty$, which suggests that the singularity at the AdS horizon remains. It is important to mention that in the case where the extra coordinate is compactified as $\bar{z} = \bar{R}z$, where \bar{R} is the compactification radius, the new domain would be $\bar{z} \in [-\pi, \pi]$, thus suppressing the singularity at the AdS horizon. In this context, the \mathbb{Z}_2 symmetry induces the presence of Dirac delta functions, located at the brane locations, in the equations of motion and consequently in the expression of the curvature scalar. This suggests that one interpretation could be that the presence of this Dirac delta distribution in the invariants does not imply a physical singularity like that produced by any diverging function, as for example in eq (3), but represents a pathology associated with mirror symmetry and the confinement of matter. It is worth mentioning that singularities of functions, in general, are not volume integrable, unlike delta distributions, which are.

B. Geodesic analysis

In this section, we will carefully analyze the geodesic movement and compare it to the results of section II. We consider the geodesic equation with $\theta = \pi/2$ and study the z and radial directions. For the z coordinate we get

$$\frac{d^2z}{d\lambda^2} - \frac{1}{z}U(\tilde{r}) \left(\frac{dt}{d\lambda} \right)^2 + \frac{1}{z}U(\tilde{r})^{-1} \left(1 - \frac{a^2}{\tilde{r}^2} \right)^{-1} \left(\frac{d\tilde{r}}{d\lambda} \right)^2 + \frac{r^2}{z} \left(\frac{d\phi}{d\lambda} \right)^2 - \frac{1}{z} \left(\frac{dz}{d\lambda} \right)^2 = 0, \quad (26)$$

where λ is an affine parameter. Also, by the very definition of geodesics, $g_{MN}\dot{x}^M\dot{x}^N = \alpha$, where $\alpha = 0$ represents null geodesics and $\alpha = -1$ time-like geodesics. Developing we obtain

$$-\frac{1}{z}U(\tilde{r})\left(\frac{dt}{d\lambda}\right)^2 + \frac{1}{z}U(\tilde{r})^{-1}\left(1 - \frac{a^2}{\tilde{r}^2}\right)^{-1}\left(\frac{d\tilde{r}}{d\lambda}\right)^2 + \frac{1}{z}\tilde{r}^2\left(\frac{d\phi}{d\lambda}\right)^2 + \frac{1}{z}\left(\frac{dz}{d\lambda}\right)^2 = \frac{z\alpha}{l^2}. \quad (27)$$

By subtracting Equations (26) and (27), we have the equation that describes the movement in the z direction,

$$\frac{d}{d\lambda}\left(\frac{1}{z^2}\frac{dz}{d\lambda}\right) = \frac{\sigma}{zl^2}, \quad (28)$$

where $\sigma = 0$ for null geodesics and $\sigma = 1$ for time-like geodesics. Equation (28) is the same equation obtained by (4), which shows that the regularization applied does not interfere with the movement in the extra direction. It is interesting to point out that this is consistent with the analysis of stability analysis in the next section. Thus, the solutions to the above equation are (5). With the same behavior as before.

We can use the geodesic equation for z to analyze the movement in the radial direction. As the metric does not depend on t and ϕ , the associated Killing vectors give the conservation of energy and angular momentum. Since $g_{00} = -l^2U(\tilde{r})/z^2$ and $g_{33} = \tilde{r}^2l^2/z^2$ (at the equator), then we get

$$\frac{dt}{d\lambda} = \frac{Ez^2}{U(\tilde{r})l^2}, \quad \frac{d\phi}{d\lambda} = \frac{Lz^2}{\tilde{r}^2l^2}. \quad (29)$$

Thus, using $z = -\frac{z_1 l}{\lambda}$ in Equation (26) and using equation (29), we have

$$\left(\frac{d\tilde{r}}{d\lambda}\right)^2 + \frac{z^4}{l^4}\left[\left(\frac{l^2}{z_1^2} + \frac{L^2}{\tilde{r}^2}\right)U(\tilde{r}) - E^2\right]\left(1 - \frac{a^2}{\tilde{r}^2}\right) = 0. \quad (30)$$

Now, it is convenient to return to the original variable r given by $\tilde{r}^2 = r^2 + a^2$. This leaves the radial equation

$$\left(\frac{dr}{d\lambda}\right)^2 + \frac{z^4}{l^4}\left[\left(\frac{l^2}{z_1^2} + \frac{L^2}{r^2 + a^2}\right)\left(1 - \frac{2M}{\sqrt{r^2 + a^2}}\right) - E^2\right] = 0 \quad (31)$$

By using the definitions (6) and (7) and defining $\bar{a} = z_1 a/l$, we get the radial equation

$$\left(\frac{d\bar{r}}{d\nu}\right)^2 + \left(1 + \frac{\bar{L}^2}{\bar{r}^2 + \bar{a}^2}\right)\left(1 - \frac{2\bar{M}}{\sqrt{\bar{r}^2 + \bar{a}^2}}\right) = \bar{E}^2. \quad (32)$$

This equation is equivalent to the radial equation of time-like geodesics with mass $\bar{M} = Mz_1/l$ and regularization parameter $\bar{a} = az_1/l$ in a Simpson-Visser like geometry [25]. According to [22], \bar{M} is the ADM mass for an observer at $z = z_0 = l^2/z_1$. Once again, we can view it as the usual radial geodesic equation $\dot{\bar{r}}^2 + V_{eff} = \bar{E}^2$. For $\bar{L} = 0$, the singularity is excluded, in comparison with (12).

We can see that the behavior near the singularity in z holds. To conclude this, it's enough to calculate the Riemann scalar in a reference frame that propagates parallel to the geodesics. Let the tangent vector to these geodesics with $L = 0$ be given by

$$u^M = \left(\frac{Ez^2}{\mathcal{U}(r)l^2}, \frac{z^2}{l^2} \sqrt{E^2 - \frac{l^2}{z_1^2} \mathcal{U}(r)}, 0, 0, \frac{z}{l} \sqrt{\frac{z^2}{z_1^2} - 1} \right), \quad (33)$$

where $\mathcal{U}(r) = 1 - \frac{2M}{\sqrt{r^2 + a^2}}$. The unit normal vector to the geodesic n^M , which is parallel propagated along it, is given by

$$n^N = \left(-\frac{zz_1}{l^2 \mathcal{U}(r)} \sqrt{E^2 - \frac{l^2}{z_1^2} \mathcal{U}(r)}, -\frac{Ez_1 z}{l^2}, 0, 0, 0 \right). \quad (34)$$

It is straightforward to check that $u^P \nabla_P n^Q = 0$. Thus, by calculating one of the curvature components in this reference frame, we obtain

$$R_{(u)(n)(u)(n)} = R_{MNPQ} u^M n^N u^P n^Q = \frac{1}{l^2} \left[1 + \frac{z^4}{2z_1^2} \left(\frac{2M}{(r^2 + a^2)^{3/2}} - \frac{6Mr^2}{(r^2 + a^2)^{5/2}} \right) \right], \quad (35)$$

which diverges along the geodesic to $\lambda \rightarrow 0^-$. Hence, our case remains regular at the origin, unlike (11); however, there is still a divergence at the AdS horizon.

IV. ENERGY CONDITIONS AND STABILITY

In this section, we will study energy conditions and stability. For this, we need of the bulk components of the energy-momentum tensor [36]. Using the components of the Einstein tensor computed previously in Eq. (17), these components are

$$\begin{aligned} \rho_E &= -\frac{1}{l^2 \kappa_5^2} \left(6 + \frac{a^2 z^2 (\tilde{r} - 4M)}{\tilde{r}^5} \right); & p_1 &= \frac{1}{l^2 \kappa_5^2} \left(6 - \frac{a^2 z^2}{\tilde{r}^4} \right); \\ p_2 &= \frac{1}{l^2 \kappa_5^2} \left(6 + \frac{a^2 z^2 (\tilde{r} - M)}{\tilde{r}^5} \right); & p_3 &= \frac{1}{l^2 \kappa_5^2} \left(6 + \frac{a^2 z^2 (\tilde{r} - 3M)}{\tilde{r}^5} \right). \end{aligned} \quad (36)$$

For $a = 0$, we have $\rho_E = -p_1 = -p_2 = -p_3 = -6/(l^2 \kappa_5^2) \equiv \Lambda_{5D}$, which is the cosmological constant term.

It is direct to check that the induced metric on the brane is given by the four-dimensional SV spacetime. The energy-momentum tensor located at the brane location $y = 0$ in the original coordinates is given by $T_\nu^\mu = \delta(y) \text{diag}(\sigma, \sigma, \sigma, \sigma)$, where σ is the brane tension. Given the absence of sources or matter fields on the brane, we can assert that the induced SV geometry on the brane should arise from the influence of the geometrical and matter deformations in the bulk. Using the junction conditions, for the line element (16), we can check that the brane tension is given by $\sigma = \frac{6}{\kappa^2 l} > 0$.

A. Energy conditions

With the expressions of the energy density and pressures obtained, we now examine if the energy conditions are globally satisfied in the bulk. In Fig. 1, we have the plot of the energy density with respect to r for a fixed point of the bulk. Analyzing the graph, it is easy to notice that ρ_E is globally negative for a fixed and finite z , thus violating the Weak Energy Condition (WEC) in this region's three cases under consideration. However, for fixed r , the energy density can assume positive values. In fact, for values r close to $r = 0$, the energy density is positive for some values of z_1 such that $|z| > z_1$.

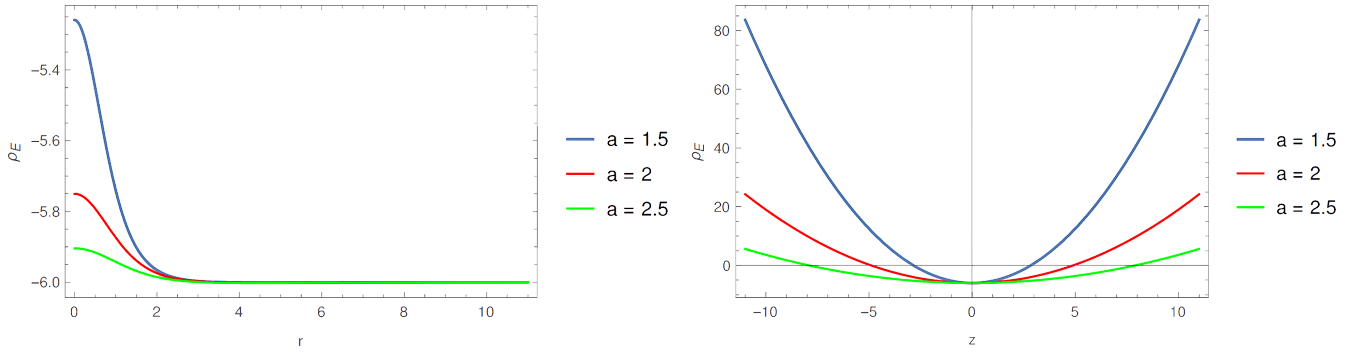


FIG. 1. Energy density ρ_E of the bulk for $l = \kappa_5 = M = z = 1$ (left) for the RBH case ($a < 2M$), OWWH case ($a = 2M$) and TWH case ($a > 2M$) and for $l = \kappa_5 = M = 1$ and $r = 0$ (right) for the RBH case ($a < 2M$), OWWH case ($a = 2M$) and TWH case ($a > 2M$).

Regarding the null energy condition (NEC), i.e., $\rho_E + p_i \geq 0$, we have the following expressions

$$\begin{aligned}\rho_E + p_1 &= -\frac{2a^2 z^2}{l^2 \kappa_5^2} \left(\frac{(r^2 + a^2)^{1/2} - 2M}{(r^2 + a^2)^{5/2}} \right), \\ \rho_E + p_2 &= \frac{3a^2 z^2}{l^2 \kappa_5^2} \cdot \frac{M}{(r^2 + a^2)^{5/2}}, \\ \rho_E + p_3 &= \frac{a^2 z^2}{l^2 \kappa_5^2} \cdot \frac{M}{(r^2 + a^2)^{5/2}}.\end{aligned}\tag{37}$$

From the above expressions, it is easy to see that NEC is satisfied for all values of r and z for $\rho_E + p_2$ and $\rho_E + p_3$. In Fig. (2) we have the plot of $\rho_E + p_1$ as a function of r for a fixed value of z , where it is possible to observe that this condition is satisfied only in a certain region only for the RBH case, and also the asymptotic radial limit of the expression $\rho_E + p_1$. Thus, from Equation (37), we can see that NEC is only satisfied in this case for $r \leq \sqrt{(2M)^2 - a^2}$, i.e., $r \leq r_h$ for the RBH case and at the limit $r \rightarrow \infty$.

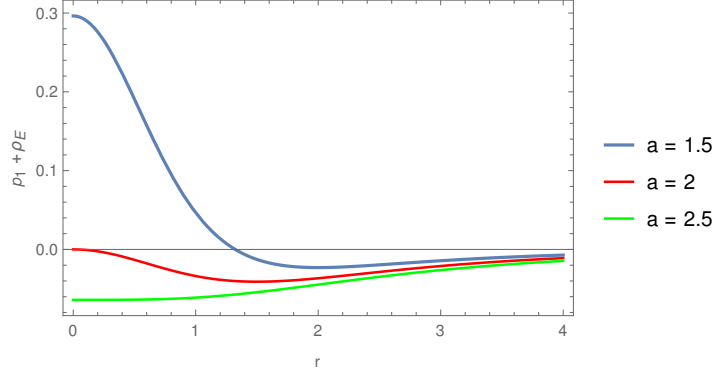


FIG. 2. $\rho_E + p_1$ of the bulk for $l = \kappa_5 = M = z = 1$ for the RBH case ($a < 2M$), OWWH case ($a = 2M$) and TWH case ($a > 2M$).

For the Strong Energy Conditions (SEC), characterized by $\rho_E + \sum_i p_i \geq 0$, we have that

$$\rho_E + \sum_i p_i = \frac{1}{l^2 \kappa_5^2} \left(18 + \frac{a^2 z^2}{\tilde{r}^5} (\tilde{r} - M) \right) \quad (38)$$

In Fig. 3, we have a plot of the above expression, when it's possible to see that equation (38) is positive when we consider a fixed point in z coordinate. In the right panel of the figure, we can see that, for adequate parameters, the expression can assume negative values.

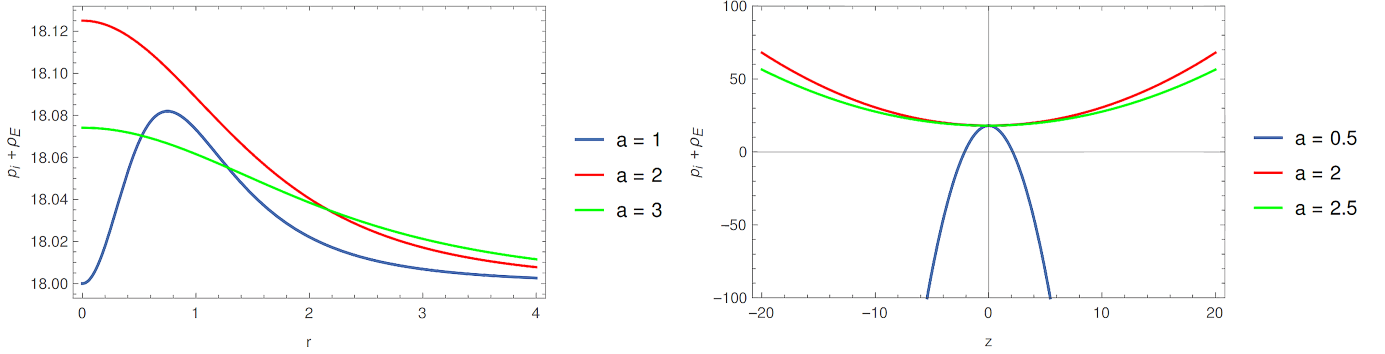


FIG. 3. In the left panel, we have $\rho_E + \sum_i p_i$ of the bulk for $l = \kappa_5 = M = z = 1$ for the RBH case ($a < 2M$), OWWH case ($a = 2M$) and TWH case ($a > 2M$), while in the right panel we have the same plot of the expression for $l = \kappa_5 = M = 1$ and $r = 0$ or the RBH case ($a < 2M$), OWWH case ($a = 2M$) and TWH case ($a > 2M$).

Thus, the energy conditions SEC are always satisfied in the bulk. While NEC and WEC may or may not be satisfied depending on the value parameters. This result differs from other braneworld models where NEC can be violated in the bulk [21].

For some parameter values, our results are consistent with observations of the shadows of M87* and the diameter of the image of Sgr A*, which have provided indications that the induced geometry on the brane could represent both ultra-compact objects and wormholes. In particular, reference [23] claims that, even though wormholes, in general, require exotic matter to remain stable, in the presence of extra dimensions such is not the case. Therefore, they showed that the wormhole solution considered does not require exotic matter on the brane.

B. Stability of the solution

We will now investigate the stability of the obtained braneworld black bounce solutions by analyzing the sound velocities of the fluid along radial and extra-dimensional directions. From equations (13) and (36) we get

$$(v_s^r)^2 = \frac{d \langle p \rangle}{d\rho} = \frac{\langle p \rangle'}{\rho'} = \frac{25M - 8\sqrt{a^2 + r^2}}{16(\sqrt{a^2 + r^2} - 5M)} \quad (39)$$

$$(v_s^z)^2 = \frac{\langle p \rangle'}{\rho'} = \frac{5M - 2\sqrt{a^2 + r^2}}{4(\sqrt{a^2 + r^2} - 4M)} \quad (40)$$

using the prime to denote the derivative with respect to coordinate r (coordinate z). We have used the fact that the average pressure $\langle p \rangle$ is given by

$$\langle p \rangle = \frac{1}{4}[p_1 + 2p_2 + p_3], \quad (41)$$

since some lateral pressures are equal. Note that v_s^i is independent of the extra-dimensional coordinate, z . This should be expected since the motion along the extra dimension is also independent of z .

As clarified at the end of section II, to ensure stability in the solution, we must impose $0 \leq (v_s^i)^2 \leq 1$, or

$$0 \leq \frac{25M - 8\sqrt{a^2 + r^2}}{16(\sqrt{a^2 + r^2} - 5M)} \leq 1; \quad 0 \leq \frac{5M - 2\sqrt{a^2 + r^2}}{4(\sqrt{a^2 + r^2} - 4M)} \leq 1. \quad (42)$$

With this, we can study the possibility of a stable solution. For traversable wormholes ($a > 2M$) with throat radii in the interval $\frac{25}{8}M \leq a \leq \frac{7}{2}M$, they are stable and physical, at least near and at the throat ($r \approx 0$). In contrast, OWWHs exhibit instability in these regions. Conversely, for RBHs, where $a < 2M$, stability and physical validity dominate in a narrow region beyond and outside the horizon. Additionally, the entirety of their inner regions fails to meet those criteria. We plot the region of stability in Fig. 4. Since we have most of the regions with instability, the

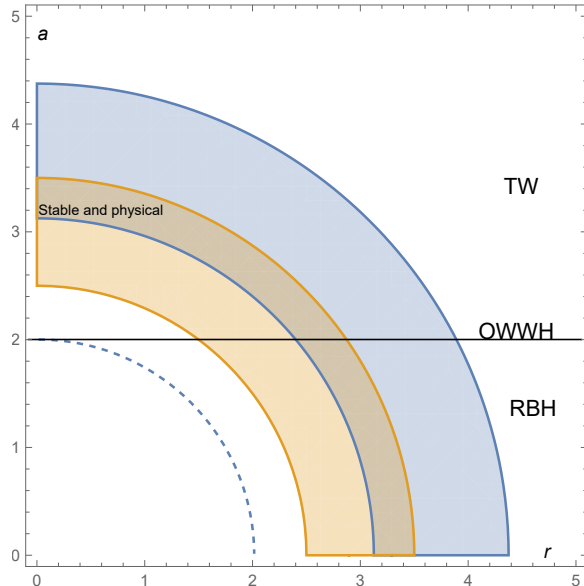


FIG. 4. Parameter space (r, a) depicting regions of stable and physical solutions, considering $M = 1$ and $a \neq 0$, for the RBH case ($a < 2M$), OWWH case ($a = 2M$), and TWH case ($a > 2M$). The dashed line denotes the RBH horizon. The superposition region between blue (along r direction) and orange (along z direction) circular sectors indicates where the sound velocities obey $0 \leq (v_s^i)^2 < 1$.

conclusion is that solutions persist to be unstable. However, it is worth noting that we have some stable regions, which is a very different result compared to the original Hawking model.

We finalize by commenting on stability under wavelength perturbations. Now we have $r_e = \sqrt{(2M_e)^2 - a^2}$, with $(2M_e)^2 > a^2$. Assuming that the AdS radius l is on the order of the Planck length, it should hold that $M/z_0 \gg 1$ to be consistent with astrophysical data. In contrast to the non-regularized solution of [22], where the spacetime is AdS everywhere, our regularized solution only exhibits AdS behavior at the asymptotic end of the radial coordinate. In our case, the spacetime is no longer flat for finite values of the radial coordinate and large values of l . Thus, it is no longer accurate to claim that the black string solution is unstable at the AdS horizon for small wavelengths. On the other hand, since our regularized solution behaves as AdS only at the asymptotic end of the radial coordinate, we can only assert that, for wavelengths much greater than l , the instability is prevented in this boundary. Although defining a proper event horizon is impossible, we can infer that this should occur far from the AdS horizon. Also, at the asymptote of the radial coordinate, the space-time behaves almost flat for wavelengths much smaller than l near the AdS horizon. Thus, this latter location could be unstable. It is worth mentioning that it becomes intriguing to test whether the regularized black string solution is unstable for finite values

of the radial coordinate and at the AdS horizon, where the space-time is no longer flat, as in the non-regularized case. This aspect could be studied in future work.

V. CONCLUSION AND SUMMARIZE

In this work, we have studied the Simpson-Visser regularization of the Randall-Sundrum Schwarzschild black hole. To accomplish this, we linearly deform the bulk geometry, represented by the $5D$ Einstein tensor, and the bulk matter distribution, represented by the $5D$ energy-momentum tensor, with respect to a coupling constant a^2 . The seed solution corresponds to the $5D$ AdS spacetime given by the black string of Hawking et.al. [22].

Moreover, both the geometrical and matter deformations, represented by equations (18) and (19) respectively, result in the induced geometry on the brane transitioning from a singular Schwarzschild spacetime to a regularized SV spacetime. Given the absence of sources or matter fields on the brane, we can assert that the induced SV geometry on the brane arises from the influence of geometrical and matter deformations in the bulk. In this context, the $5D$ spacetime is regular at the origin $r = 0$ (or $\tilde{r} = a$), unlike [22], where singularity occurs at the origin. However, the singularity at the AdS horizon persists. This latter singularity could be suppressed in a scenario where the extra dimension is compactified.

Despite being asymptotically AdS, the above deformation induces a transition from a vacuum distribution to an anisotropic distribution. This behavior differs from the black string of Hawking et.al, which is globally AdS[22]. In fact, by studying the energy conditions, we found that the NEC and SEC are always satisfied in bulk, while the WEC may or may not be satisfied depending on the values of the parameters. This result differs from other Brane world models, where the NEC can be violated in bulk [21]. An interesting result is that, for some parameter values, our results are consistent with observations of the shadows of M87* and the diameter of the image of Sgr A*, which have provided indications that the induced geometry on the brane could represent both ultra-compact objects and wormholes. In particular, reference [23] claims that even though wormholes generally require exotic matter to remain stable, such is not the case in the presence of extra dimensions. Therefore, they showed that the wormhole solution considered does not require exotic matter on the brane.

We have also scrutinized the stability (and physical validity) of the braneworld black-bounce solutions in bulk by evaluating the sound speed of the source along the r and z directions. Our analysis unveiled specific regions where stability and physicality are guaranteed for both wormhole

and regular black hole solutions, contingent upon the bounce parameter a , as shown in Fig. 4. It is worth noting that in braneworld models where $a = 0$, there are no stable regions. Because the spacetime is only AdS at the asymptote of the radial coordinate, we can assert that only at that location the solution is unstable considering now wavelength perturbations near the AdS horizon but stable far from it. Thus, it becomes intriguing to test whether our solution is unstable for finite values of the radial coordinate, where the spacetime is no longer AdS as the black string of reference [22].

Finally, we mention that in the case of the coordinate z , we cannot do a Simpson-Visser-like regularization $z \rightarrow \sqrt{z^2 + b^2}$, as we would continue to have a divergence in $z \rightarrow \infty$. An alternative would be to consider an exchange of the type $z \rightarrow f_b(z)$ so that $\lim_{z \rightarrow \infty} f_b(z)$ is a constant and $\lim_{b \rightarrow 0} f_b(z) = z$. However, nothing guarantees that such a function exists, and if it does, imposing an analytical form for $f_b(z)$ does not seem to be trivial. It is also necessary to test whether the regularized black string solution is unstable for finite values of the radial coordinate and at the AdS horizon, where the space-time is no longer flat, as in the non-regularized case. These aspects will be explored in future work.

-
- [1] B. P. Abbott *et al.* (LIGO Scientific, Virgo), “Observation of Gravitational Waves from a Binary Black Hole Merger,” *Phys. Rev. Lett.* **116**, 061102 (2016), arXiv:1602.03837 [gr-qc].
 - [2] Kazunori Akiyama *et al.* (Event Horizon Telescope), “First Sagittarius A* Event Horizon Telescope Results. I. The Shadow of the Supermassive Black Hole in the Center of the Milky Way,” *Astrophys. J. Lett.* **930**, L12 (2022), arXiv:2311.08680 [astro-ph.HE].
 - [3] Kazunori Akiyama *et al.* (Event Horizon Telescope), “First M87 Event Horizon Telescope Results. I. The Shadow of the Supermassive Black Hole,” *Astrophys. J. Lett.* **875**, L1 (2019), arXiv:1906.11238 [astro-ph.GA].
 - [4] B. P. Abbott *et al.* (LIGO Scientific, Virgo), “GW170817: Observation of Gravitational Waves from a Binary Neutron Star Inspiral,” *Phys. Rev. Lett.* **119**, 161101 (2017), arXiv:1710.05832 [gr-qc].
 - [5] N. Aghanim *et al.* (Planck), “Planck 2018 results. VI. Cosmological parameters,” *Astron. Astrophys.* **641**, A6 (2020), [Erratum: *Astron. Astrophys.* 652, C4 (2021)], arXiv:1807.06209 [astro-ph.CO].
 - [6] Simone Aiola *et al.* (ACT), “The Atacama Cosmology Telescope: DR4 Maps and Cosmological Parameters,” *JCAP* **12**, 047 (2020), arXiv:2007.07288 [astro-ph.CO].
 - [7] James E. Gunn *et al.* (SDSS), “The 2.5 m Telescope of the Sloan Digital Sky Survey,” *Astron. J.*

- 131**, 2332–2359 (2006), arXiv:astro-ph/0602326.
- [8] Lisa Randall and Raman Sundrum, “A Large mass hierarchy from a small extra dimension,” *Phys. Rev. Lett.* **83**, 3370–3373 (1999), arXiv:hep-ph/9905221.
- [9] Lisa Randall and Raman Sundrum, “An Alternative to compactification,” *Phys. Rev. Lett.* **83**, 4690–4693 (1999), arXiv:hep-th/9906064.
- [10] Luca Visinelli, Nadia Bolis, and Sunny Vagnozzi, “Brane-world extra dimensions in light of GW170817,” *Phys. Rev. D* **97**, 064039 (2018), arXiv:1711.06628 [gr-qc].
- [11] Sunny Vagnozzi and Luca Visinelli, “Hunting for extra dimensions in the shadow of M87*,” *Phys. Rev. D* **100**, 024020 (2019), arXiv:1905.12421 [gr-qc].
- [12] Tetsuya Shiromizu, Kei-ichi Maeda, and Misao Sasaki, “The Einstein equation on the 3-brane world,” *Phys. Rev. D* **62**, 024012 (2000), arXiv:gr-qc/9910076.
- [13] C. Molina and J. C. S. Neves, “Wormholes in de Sitter branes,” *Phys. Rev. D* **86**, 024015 (2012), arXiv:1204.1291 [gr-qc].
- [14] J. C. S. Neves, “Note on regular black holes in a brane world,” *Phys. Rev. D* **92**, 084015 (2015), arXiv:1508.03615 [gr-qc].
- [15] J. C. S. Neves and C. Molina, “Rotating black holes in a Randall-Sundrum brane with a cosmological constant,” *Phys. Rev. D* **86**, 124047 (2012), arXiv:1211.2848 [gr-qc].
- [16] Roberto Casadio, Jorge Ovalle, and Roldão da Rocha, “The Minimal Geometric Deformation Approach Extended,” *Class. Quant. Grav.* **32**, 215020 (2015), arXiv:1503.02873 [gr-qc].
- [17] P. Kanti, I. Olasagasti, and K. Tamvakis, “Schwarzschild black branes and strings in higher dimensional brane worlds,” *Phys. Rev. D* **66**, 104026 (2002), arXiv:hep-th/0207283.
- [18] Simon Creek, Ruth Gregory, Panagiota Kanti, and Bina Mistry, “Braneworld stars and black holes,” *Class. Quant. Grav.* **23**, 6633–6658 (2006), arXiv:hep-th/0606006.
- [19] Theodoros Nakas, Panagiota Kanti, and Nikolaos Pappas, “Incorporating physical constraints in braneworld black-string solutions for a minkowski brane in scalar-tensor gravity,” *Physical Review D* **101** (2020), 10.1103/physrevd.101.084056.
- [20] Theodoros Nakas, Thomas D. Pappas, and Zdeněk Stuchlík, “Bridging dimensions: General embedding algorithm and field-theory reconstruction in 5D braneworld models,” *Phys. Rev. D* **109**, L041501 (2024), arXiv:2309.00873 [gr-qc].
- [21] Juliano C. S. Neves, “Five-dimensional regular black holes in a brane world,” *Phys. Rev. D* **104**, 084019 (2021), arXiv:2107.04072 [hep-th].

- [22] A. Chamblin, S. W. Hawking, and H. S. Reall, “Brane world black holes,” *Phys. Rev. D* **61**, 065007 (2000), arXiv:hep-th/9909205.
- [23] Indrani Banerjee, Sumanta Chakraborty, and Soumitra SenGupta, “Hunting extra dimensions in the shadow of Sgr A*,” *Phys. Rev. D* **106**, 084051 (2022), arXiv:2207.09003 [gr-qc].
- [24] R. Gregory and R. Laflamme, “Black strings and p-branes are unstable,” *Phys. Rev. Lett.* **70**, 2837–2840 (1993), arXiv:hep-th/9301052.
- [25] Alex Simpson and Matt Visser, “Black-bounce to traversable wormhole,” *JCAP* **02**, 042 (2019), arXiv:1812.07114 [gr-qc].
- [26] Job Furtado and Geová Alencar, “BTZ Black-Bounce to Traversable Wormhole,” *Universe* **8**, 625 (2022), arXiv:2210.06608 [gr-qc].
- [27] Arthur Menezes Lima, Geová Maciel de Alencar Filho, and Job Saraiva Furtado Neto, “Black String Bounce to Traversable Wormhole,” *Symmetry* **15**, 150 (2023), arXiv:2211.12349 [gr-qc].
- [28] A. Lima, G. Alencar, R. N. Costa Filho, and R. R. Landim, “Charged black string bounce and its field source,” *Gen. Rel. Grav.* **55**, 108 (2023), arXiv:2306.03029 [gr-qc].
- [29] A. Lima, G. Alencar, and Diego Sáez-Chillon Gómez, “Regularizing rotating black strings with a new black-bounce solution,” *Phys. Rev. D* **109**, 064038 (2024), arXiv:2307.07404 [gr-qc].
- [30] G. Alencar, Kirill A. Bronnikov, Manuel E. Rodrigues, Diego Sáez-Chillón Gómez, and Marcos V. de S. Silva, “On black bounce space-times in non-linear electrodynamics,” (2024), arXiv:2403.12897 [gr-qc].
- [31] Kirill A. Bronnikov, Manuel E. Rodrigues, and Marcos V. de S. Silva, “Cylindrical black bounces and their field sources,” *Phys. Rev. D* **108**, 024065 (2023), arXiv:2305.19296 [gr-qc].
- [32] Jorge Ovalle, “Decoupling gravitational sources in general relativity: from perfect to anisotropic fluids,” *Phys. Rev. D* **95**, 104019 (2017), arXiv:1704.05899 [gr-qc].
- [33] Ruth Gregory, “Black string instabilities in Anti-de Sitter space,” *Class. Quant. Grav.* **17**, L125–L132 (2000), arXiv:hep-th/0004101.
- [34] Panagiota Kanti and Kyriakos Tamvakis, “Quest for localized 4-D black holes in brane worlds,” *Phys. Rev. D* **65**, 084010 (2002), arXiv:hep-th/0110298.
- [35] Salvatore Capozziello and Nisha Godani, “Non-local gravity wormholes,” *Phys. Lett. B* **835**, 137572 (2022), arXiv:2211.06481 [gr-qc].
- [36] Pierre Binétruy, Cedric Deffayet, and David Langlois, “Nonconventional cosmology from a brane universe,” *Nucl. Phys. B* **565**, 269–287 (2000), arXiv:hep-th/9905012.